LETTER

Automatic Mura Detection for Display Film Using Mask Filtering in Wavelet Transform

Jong-Seung PARK[†], ***Student Member and*** **Seung-Ho LEE**[††a)], ***Nonmember***

SUMMARY In this letter, we present a method for automatic mura detection for display film using the efficient decision of cut-off frequency with DCT and mask filtering with wavelet transform. First, the background image including reflected light is estimated using DCT with adaptive cut-off frequency, and DWT is applied to background-removed images for generating mura mask. Then, a mura mask is generated by separating low-frequency noise in the approximation coefficients. Lastly, mura is detected by applying mura mask filtering to the detail coefficients. According to the comparison by Semu index, the results from the proposed method are superior to those from the existing methods. This indicates that the proposed method is high in reliability.

key words: *machine vision, mura detection, mura mask, mask filtering*

1. Introduction

These days, the demand for flat panel displays (FPDs) is increasing with the expansion of smart phone and tablet PC markets. Accordingly, the needs of quality inspection of a display film in FPD manufacturing process is increasing to an automatic method for detecting defects. In general, the quality inspection of display film is performed by a machine vision system. However, such systems fail to detect low-contrast defects. For this reason, precise quality inspection is still performed by the naked eye. According to the Semiconductor Equipment and Materials International (SEMI) Standards, mura refers to a defect indicated by a local brightness change that disturbs human vision [1]. SEMI specifies SEMU as a measurement index to evaluate objective reliability [2].

There are various existing methods for detecting mura, such as removing the background image [3]–[7] and using mura features [8], [9]. To detect mura by removing the background image, Lu and Tsai [3], [4] and Wang et al. [5] proposed a method for estimating the background image using singular value decomposition (SVD). This method is very sensitive to pattern directivity, thus making it possible to remove mura features as well. Lee and Yoo [6] proposed a method for estimating the background image using the modified regression diagnostics and Niblack's thresholding method. This method is suitable for detecting extended mura, but not spot mura. To detect mura by using mura features, Bi et al. [8] proposed a method using the level set method based on modified active contour. This method requires many calculations, making detection slow, and changes parameters according to image contrast. Li and Tsai [9] proposed a method for detecting mura by applying threshold values to a distance between a direct line decided by modified hough transform and pixel value of the input image. However, this method has a weak point that the limited range of Hough transform parameter has to be redecided according to images.

In this paper, we propose an automatic inspection method to detect mura defect. The proposed method consists of three stages: In the first stage, the background image including reflected light is estimated using discrete cosine transform (DCT) with adaptive cut-off frequency and discrete wavelet transform (DWT) is applied to background-removed images for generating mura mask. In the second stage, a mura mask free of low-frequency noise is generated by applying the region-growth method to the approximation coefficients. In the third stage, mura is detected by applying mura mask filtering to the detail coefficients to emphasize mura and remove high-frequency noise.

2. Automatic Mura Detection Method

2.1 Summary of Proposed Method

Figure 1 illustrates a summary of the proposed automatic mura detection method. In the first stage, the background image is removed using DCT [10] to minimize the influence of illumination, and DWT [11] is applied to analyze the background-removed image in spatial and frequency domains. In the second stage, mura seed points and mura region image are generated by binarizing the approximation coefficients on the basis of standard deviation, and mura masks are generated by adding 8-connected pixels to mura seed points. In the third stage, mura mask filtering is performed using generated mura masks. Mura features are emphasized and high-frequency noise is removed from each detail coefficient. The mura-emphasized image is generated by applying inverse discrete wavelet transform (IDWT) to the filtered wavelet coefficients. Lastly, Semu evaluation is performed with the defect level of the mura detected image.

Manuscript received July 10, 2014.
Manuscript revised November 5, 2014.
Manuscript publicized November 21, 2014.

[†]The author is with the Department of Electronic Engineering, Hanbat National University, 125 Dongseo-daero, Yuseong-gu, Daejeon, 305–719 Korea.

[††]The author is with the Department of Electronics & Control Engineering, Hanbat National University, 125, Dongseo-daero, Yuseong-gu, Daejeon, 305–719 Korea.

a) E-mail: shlee@cad.hanbat.ac.kr (Corresponding author)

DOI: 10.1587/transinf.2014EDL8140

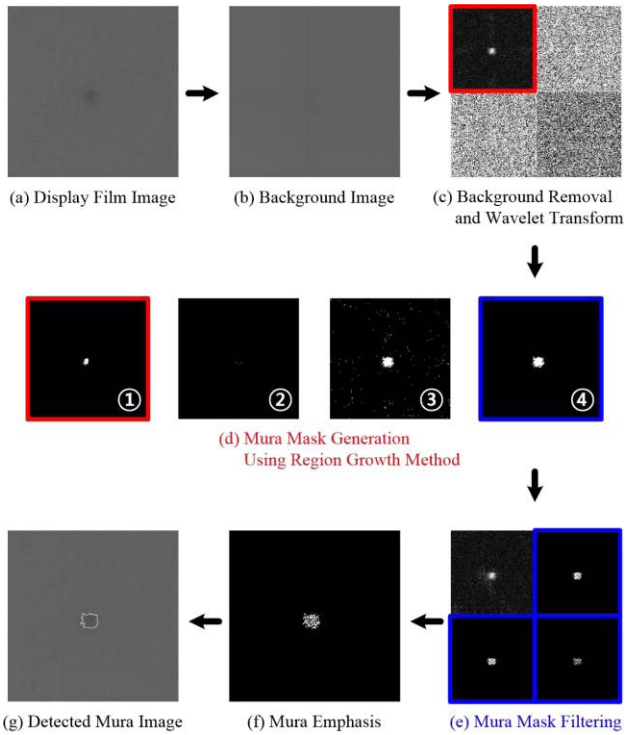

Fig. 1 Summary of proposed method.

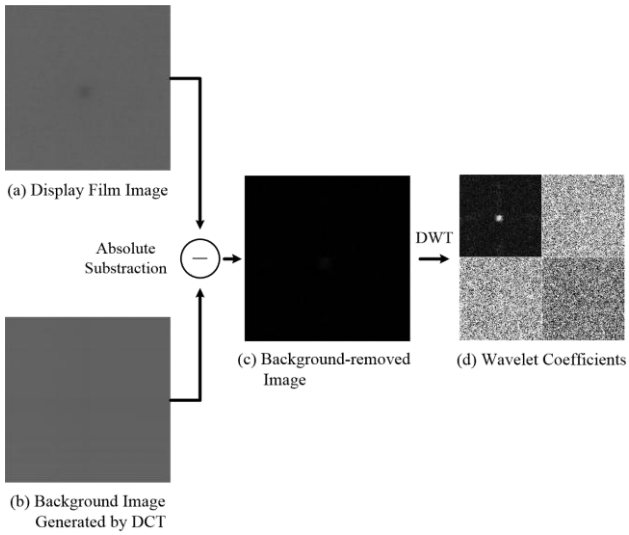

Fig. 2 Background image removal by DCT and DWT.

2.2 Background Removal and DWT Application Using DCT

The horizontal and vertical DCT coefficients are only used to estimate the background image including reflected light in automatic inspection process. Cutoff frequency is decided by using moving average of the rate of change to separate the main and sub components of the horizontal and vertical DCT coefficients with adaptive manner. The following shows the cutoff frequencies.

$$\begin{cases} F_u = u, & \dfrac{1}{10}\displaystyle\sum_{u=x}^{x+9}\left|C(u+1,0)-C(u,0)\right| < 1 \\ F_v = v, & \dfrac{1}{10}\displaystyle\sum_{v=y}^{y+9}\left|C(0,v+1)-C(0,v)\right| < 1 \end{cases} \tag{1}$$

Where F_u is the horizontal cutoff frequency, F_v is the vertical cutoff frequency, and $C(u,0)$ is the horizontal DCT coefficient, $C(0,v)$ is the vertical DCT coefficient, $x = 1, 11, 21, \cdots, M-9$, $y = 1, 11, 21, \cdots, N-9$.

The following shows the filter of the horizontal and vertical DCT coefficients with the cutoff frequency.

$$\begin{aligned} C(u,0) &= \begin{cases} C(u,0), & u < F_u \\ 0, & otherwise \end{cases} \\ C(0,v) &= \begin{cases} C(0,v), & v < F_v \\ 0, & otherwise \end{cases} \end{aligned} \tag{2}$$

The background image is generated by applying IDCT to the DCT coefficients filtered by adaptive cutoff frequency. The background image is removed from the original image by absolute subtraction between original and background images. DWT is applied to the background-removed image to analyze those in spatial and frequency domains. Figure 2 illustrates a process of removing the background image using DCT and applying DWT to them.

2.3 Mura Mask Generation

The approximation coefficients generated by DWT, which are LL sub-bands of DWT, have features of the background-removed image. The background-removed image includes mura features as well as some features of remained background even after the removal of background information. Because some features of remained background can be the low-frequency noise, the threshold value is decided using standard deviation to remove the low-frequency noise included in the approximation coefficients. The following shows the threshold.

$$\begin{aligned} th_{mask} &= m + \beta\sigma \\ &= m + \beta\sqrt{\frac{1}{MN}\sum_{x=0}^{M-1}\sum_{y=0}^{N-1}(W_\phi(x,y)-m)^2} \end{aligned} \tag{3}$$

Where $W_\phi(x,y)$ is the approximation coefficients, m is the average of the approximation coefficients, and $\beta = 1, 2, \cdots, 6$.

The following shows the binarization of the approximation coefficients with a decided threshold value.

$$W_\phi(x,y) = \begin{cases} 1, & th_{mask} \geq W_\phi(x,y) \\ 0, & otherwise \end{cases} \tag{4}$$

Proposed algorithm to remove low-frequency noise and generate mura mask by applying region-growth method to the approximation coefficients is as follows.

1. The mura seed image is generated on the basis of

$th_{mask}(\beta = 6)$.

2. A mura seed point is generated by eroding a connected component in a generated area with a pixel.
3. Based on $th_{mask}(\beta = 3)$, the mura region image is generated in which no mura features are lost.
4. Mura mask is generated by adding 8-connected pixels to mura seed point.

A generated mura mask becomes an object which is completely separated from low-frequency noise included in the approximation coefficients. Figure 3 illustrates a process of generating mura mask.

2.4 Mura Mask Filtering

The detail coefficients generated by DWT, which are LH, HL, HH sub-bands of DWT, have horizontal, vertical and diagonal high-frequency components of the background-removed image. High-frequency components include not only high-frequency components of mura features but also high-frequency components of remained background features even after the removal of background information. High-frequency components of remained background features can be the high-frequency noise. To remove such high-frequency noise, mura mask filtering is performed by applying generated mura mask to each detail coefficient. The mask-on component is emphasized as mura features, while the mask-off component is removed as high-frequency noise. The following shows mura mask filtering.

$$W_{\psi}^{i}(x,y) = \begin{cases} \alpha \times W_{\psi}^{i}(x,y), & mask-on \\ 0, & mask-off \end{cases} \tag{5}$$

Where $W_{\psi}^{i}(x,y)$ is the detail coefficient, α is the constant, and $i = H, V, D$.

The mura-emphasized image is generated by applying IDWT to the filtered wavelet coefficients. The mura-emphasized image is made into an object connected with mura by applying morphological closing operation, and the mura-detected image is generated by illustrating the object's contour in the original image. Figure 4 illustrates a process of mura mask filtering.

3. Experimental Results

In this experiment, 200 gray scale images with 410×410 pixels were used to calculate a detection rate of the proposed method. The result showed a detection rate of 95.5% with 191 detected images and 9 undetected images.

The detected mura defect is quantized by Semu defined as measurement index in the SEMI standards to evaluate the objective reliability of the proposed method [2]. A lower Semu value means a mura defect more difficult to detect. Semu is defined as follows.

$$Semu = \frac{|C_x|}{C_{jnd}} = \frac{\left|\frac{I_M - I_B}{I_B}\right|}{\left(\frac{1.97}{S_x^{0.33}} + 0.72\right)} \tag{6}$$

Where C_x is the average contrast of mura being measured, C_{jnd} is the contrast of mura at JND, I_M is the average gray level of mura region, I_B is the average gray level of background region, and S_x is the surface area of mura being measured.

The experiment used similar sample images generated to compare the proposed method with the Semu evaluation results of Chen and Kuo [7]. Figure 5 illustrates the results from detecting mura with the proposed method using sample images which has the gray level difference between mura

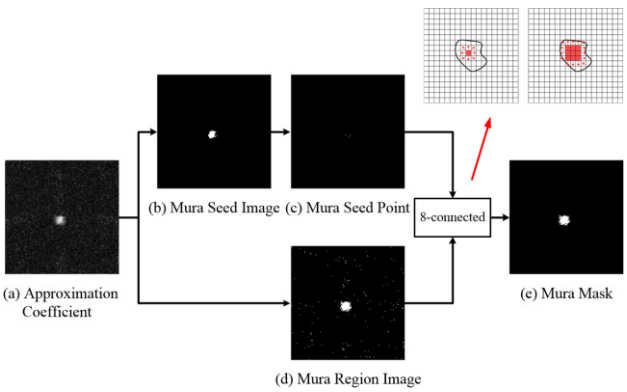

Fig. 3 Mura mask generation process.

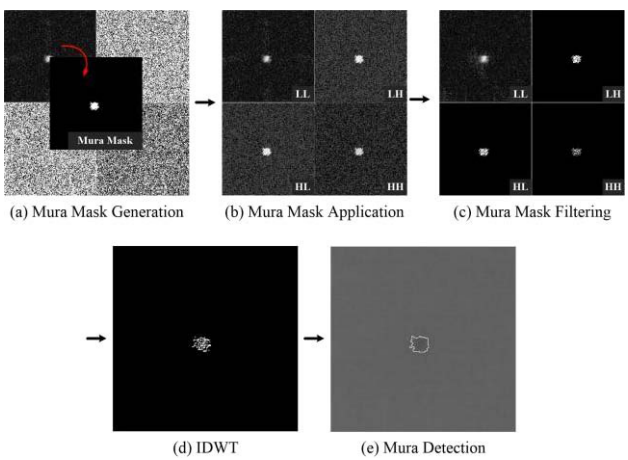

Fig. 4 Mura mask filtering process.

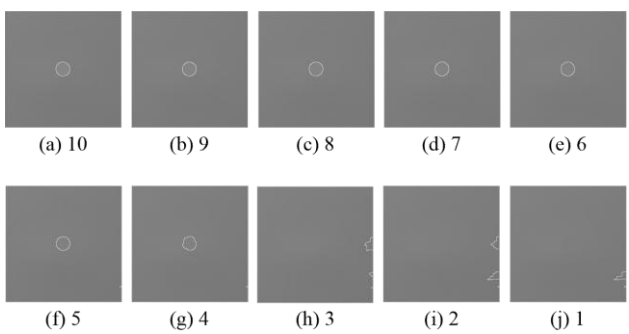

Fig. 5 Mura detection results for sample images.

Table 1 Comparison between proposed method and chen and Kuo's Semu evaluation results.

Gray level difference	C_x		C_{jnd}		Semu		Inspection quality	
	Proposed	Chen & Kuo	Proposed	Chen & Kuo	Proposed	Chen & Kuo	Proposed	Chen & Kuo
10	8.16	8.32	0.88	0.88	9.24	9.30	Good	Good
9	7.36	7.42	0.88	0.88	8.33	8.39	Good	Good
8	6.57	6.61	0.88	0.88	7.43	7.48	Good	Good
7	5.75	5.79	0.88	0.88	6.51	6.55	Good	Good
6	4.96	4.78	0.88	0.88	5.61	5.39	Good	Good
5	4.15	3.07	0.88	0.89	4.70	3.44	Good	Good
4	3.34	0.52	0.89	1.22	3.77	0.43	Good	Fail
3	1.93	0.48	0.93	1.28	2.08	0.31	Fail	Fail
2	2.34	0.37	0.90	1.28	2.60	0.29	Fail	Fail
1	2.74	0.18	0.96	1.50	2.85	0.12	Fail	Fail

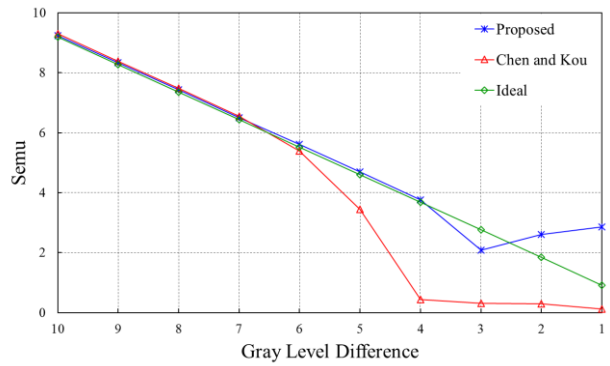

Fig. 6 Distribution of Semu values calculated using the proposed method, Chen & Kuo's method and the sample images generation conditions.

and background from 10 to 1.

Table 1 shows the results of Semu evaluation between the proposed method and Chen and Kuo's method. Similar results are represented by gray level differences 10 to 6.

Figure 6 illustrates the distribution of Semu values calculated using the proposed method, Chen and Kuo's method and the sample images generation conditions. Up to gray level difference 4, the proposed method corresponded to the sample images generation conditions in Semu values. Up to gray level difference 6, Chen and Kuo corresponded to the sample images generation conditions in Semu values. The proposed method was excellent.

4. Conclusion

In this paper, we proposed a method for automatic mura detection in display films by using artificial light to remove background noise in an automatic inspection process, using adaptive cutoff frequency in DCT, and performing mask filtering in DWT. By mura mask filtering, the method emphasizes mura features and removes high-frequency noise, thus making it possible to detect mura well in images that have low contrast which has a low contrast between mura and background. The results were superior to those of the existing methods according to the Semu evaluation of detected mura. This indicates that the proposed method is high in reliability.

References

[1] K. Taniguchi, K. Ueta, and S. Tatsumi, "A mura detection method," Pattern Recognition, vol.39, pp.1044–1052, 2006.
[2] "Definition of measurement index (SEMU) for luminance Mura in FPD image quality inspection," SEMI D31-1102, 2002.
[3] C.J. Lu and D.M. Tsai, "Defect inspection of patterned thin film transistor-liquid crystal display panels using a fast sub-image-based singular value decomposition," Int. J. Production Research, vol.42, no.20, pp.4331–4351, 2004.
[4] C.J. Lu and D.M. Tsai, "Automatic defect inspection for LCDs using singular value decomposition," Int. J. Advanced Manufacturing Technology, vol.25, pp.53–61, 2005.
[5] J.W. Wang, W.Y. Chen, and J.S. Lee, "Singular value decomposition combined with wavelet transform for LCD defect detection," IEEE Electron. Lett., vol.48, pp.266–267, 2012.
[6] J.Y. Lee and S.I. Yoo, "Automatic detection of region-mura defect in TFT-LCD," IEICE Trans. Inf. & Syst., vol.E87-D, no.10, pp.2371–2378, Oct. 2004.
[7] L.C. Chen and C.C. Kuo, "Automatic TFT-LCD mura defect inspection using discrete cosine transform-based background filtering and 'just noticeable difference' quantification strategies," Measurement Science and Technology, vol.19, pp.1–10, 2008.
[8] X. Bi, C. Zhuang, and H. Ding, "A new mura defect inspection way for TFT-LCD using level set method," IEEE Signal Process. Lett., vol.16, no.4, pp.311–314, 2009.
[9] W.C. Li and D.M. Tsai, "Defect inspection in low-contrast LCD images using Hough transform-based nonstationary line detection," IEEE Trans. Industrial Informatics, vol.7, no.1, pp.136–147, 2011.
[10] S.A. Khayam, "The discrete cosine transform (DCT): Theory and application," Seminar Note, Department of Electrical & Computing Engineering Michigan State University, 2003.
[11] R.C. Gonzalez and R.E. Woods, Digital Image Processing, 3rd ed., Prentice Hall, 2008.